FINE-SCALE ACTIVITY IN A TURBULENT CYLINDER WAKE

Anton Vernet

Departament d'Enginyeria Mecànica, ETSEQ, Universitat Rovira i Virgili,

Crta. Salou s/n, 43006, Tarragona, Spain
avernet@etseq.urv.es

Josep A. Ferré

Departament d'Enginyeria Mecànica, ETSEQ, Universitat Rovira i Virgili,

Crta. Salou s/n, 43006, Tarragona, Spain
jaferre@etseq.urv.es

ABSTRACT

A Fine-Scale Turbulence Indicating Function (FSTIF) is used to obtain the incoherent footprints of the large-scale motions (Karman vortices) in a turbulent cylinder wake. FSTIF is compared with the streamwise and lateral incoherent normal stresses and with the Reynolds incoherent stress derived from the triple decomposition of velocity signals, which have been low-pass filtered with several cut-off frequencies. Results show that most of the contribution to the incoherent stresses computed from the triple decomposition is mainly due to low-frequency differences between individual events rather than to a fine scale (high frequency) activity. Therefore, the FSTIF seems to be better suited to analyse the true fine scale activity of turbulence.

INTRODUCTION

The triple decomposition of the velocity field (Hussain, 1983) can be used to analyse the large-scale/fine-scale activity of turbulent flows. Using this decomposition each component of the total instantaneous velocity, u_i, is considered to be the sum of the long time-averaged mean, $\overline{U}_i$, the coherent velocity, u_{ic} and the incoherent velocity fluctuations, u_{ir}, such that

$$u_i(x,y,z,t) = \overline{U}_i(x,y) + u_{ic}(x,y,z) + u_{ir}(x,y,z,t) \qquad (1)$$

Therefore, the incoherent or small-scale velocity can be computed as the difference between the instantaneous velocity fluctuations ($u_i - \overline{U}_i$) and the coherent velocity, i.e. $u_{ir} = (u_i - \overline{U}_i) - u_{ic}$, where u_{ic} is some properly defined ensemble average. In this paper, a pattern recognition (PR) technique (Ferré and Giralt, 1989) is used to obtain the coherent velocity associated to the passage of the large-scale structures (Karman vortices). On the frame of triple decomposition, one way to evaluate the fine scale activity of these coherent motions is to analyse the contours of the stresses due to the incoherent (random) motions. These random components can be calculated from the difference between the total stress and the coherent stress,

$$< u_r^2 > = < u^2 > - < u >^2 \qquad (2)$$

$$< v_r^2 > = < v^2 > - < v >^2 \qquad (3)$$

$$< uv_r > = < uv > - < u >< v > \qquad (4)$$

In these equations and in the rest of the paper the symbols < > are used to represent an ensemble average, thus $< u >$ is equivalent to u_c. Even that this seems to be a good indicator of the fine scale activity, this procedure must be interpreted with caution. As pointed out by Antonia et al. (1987) and by Ferré et al. (1990), in fully developed turbulent flows the large-scale structures can present differences in size, intensity and orientation not necessarily related to the smaller turbulence scales. Misclassifications and misalignments during the identification could also occur. All of these factors will affect the values and shape of the contours of random components. To gain a better understanding of the fine scale activity free of these drawbacks, Ferré et al. (1990) used a fine-scale turbulence indicating function (FSTIF), that they defined as the envelope of the second time derivative of velocity. The aim of this paper to compare the performance of the triple decomposition and the FSTIF in detecting the fine-scale activity in a turbulent flow. To do this analysis the raw velocity signals are low-pass filtered with decreasing cut-off frequencies, in order to reduce their high-frequency components, and the

output from triple decomposition and FSTIF analysis of these signals are compared.

EXPERIMENTAL SET-UP

The experimental data has been obtained in a wind tunnel that has a test section of 600x600 mm and 3m long. A uniform free-stream velocity of U_0=9.0 m/s was used so that the Reynolds number, based on the nominal cylinder diameter (D=11.6mm) was Re=7000.

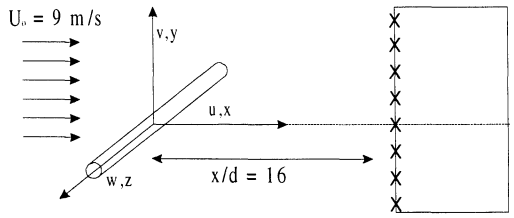

Figure1: Definition sketch.

Measurements have been made at x/D=16 with a rake of eight X-wires, placed in a vertical plane positioned at the centre of the wake, as show in figure 1. Spacing between adjacent probes was 7mm. The spatial co-ordinates are normalised according to $x^* = -U_0 t / l_0$ and $y^* = y/l_0$, where $y = l_0 = 11.6$ mm is the lateral location where the mean velocity defect is half of its maximum value. The streamwise location x/D=16 has been chosen because in this position the large-scale structures (Karman vortices) are still well defined but the finer scales of turbulence are already developed. The output voltages of the anemometers were low-pass filtered at 2.5kHz and sampled at 5kHz per channel during 40 seconds. The nominal shedding frequency of the Karman vortices is 156Hz, therefore 40 seconds of data account for more than 6000 Karman vortices and yield accurate first and second order statistics.

ANALYSIS OF NON-FILTERED DATA

Pattern recognition technique

To obtain the ensemble average of the velocity footprints of the Karman vortices embedded in the turbulent signals the PR technique has been used. This technique is based on the computation of the cross-correlation between an initial template (Figure 2a) and the instantaneous velocity signal obtained in one experiment. Values of the cross-correlation larger than some threshold identifies the occurrence of individual events similar to the initial velocity template. Then the selected events are ensemble averaged to obtain the coherent velocity components. The procedure is iterated using the ensemble average as the template for the next iteration until there is no further change between the ensemble average and the template. The iterative process removes the bias that may be introduced through the selection of the initial template. In the present work only four iterations were required to achieve convergence. While the ensemble averages displayed span from x*=0 to x*=8, only the central part of the template, from x*=2 to x*=6, was used to compute the correlation coefficient in order not to bias the ensemble average towards periodicity.

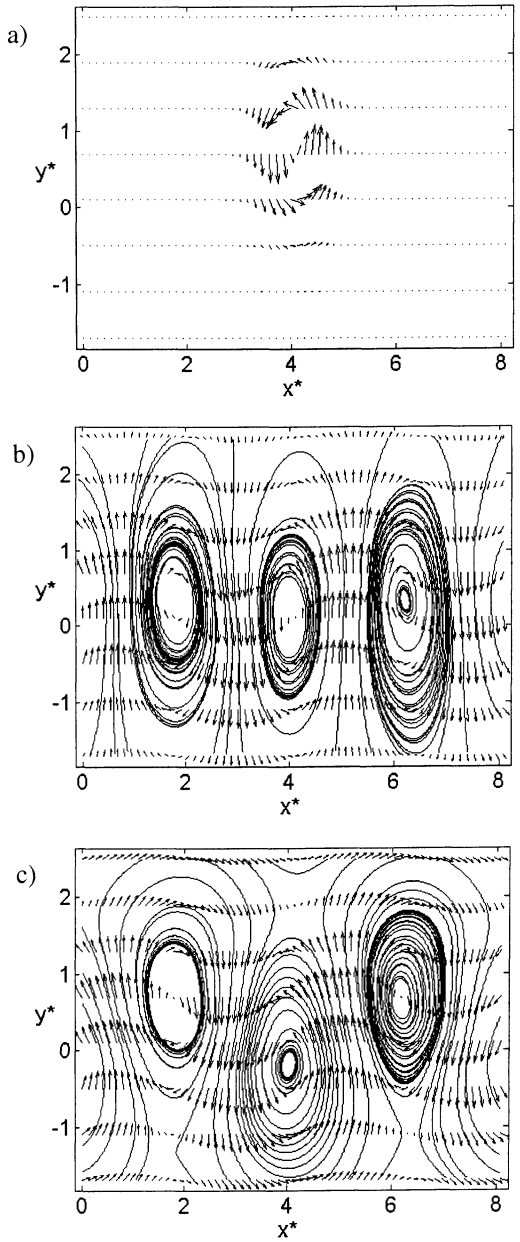

Figure2: a) Initial template, b) ensemble average and c) ensemble average with mean profile added.

Figure 2b shows the ensemble average of the velocity fluctuations associated to the passage of Karman vortices. Figure 2c shows the same ensemble average after the streamwise mean

velocity profile has been added, and a convection velocity $U_c=0.9U_o$ has been subtracted in order to display the Karman vortices as they could be seen by an observer moving at U_c. Pathlines have been added to show circulation. In this figure and in the rest of the paper the flow is moving from left to right. A total number of 4629 individuals have been averaged in figures 2b and 2c, which represents almost the 70% of the Karman vortices shed by the cylinder.

The spectrum of the *v*-velocity component (figure 3) at y* = 1.3, near the location of maximum shear, shows a peak frequency at f=156 that corresponds to a Strouhal number (St=f *D/U_o) of 0.2, and a well-developed Kolmogorof inertial range.

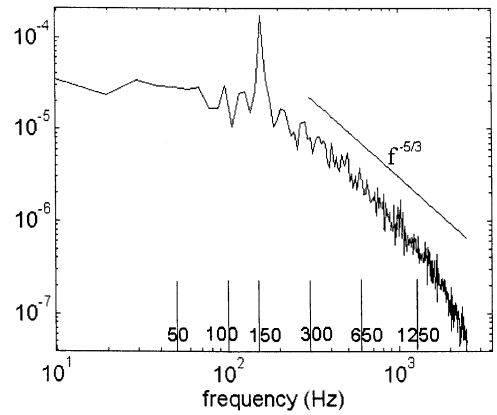

Figure 3: The v-velocity spectrum at y*= 1.3

The random stresses $< u_r^2 >$, $< v_r^2 >$ and $< uv_r >$ corresponding to the structure obtained by PR analysis are presented in figures 4a, b and c, respectively. Figures 4a and 4b show that the maxima of $< u_r^2 >$ and $< v_r^2 >$ are located over the foci centres of the Karman vortices. However, the $< uv_r >$ (figure 4c) shows alternate positive and negative lobes in each side of the wake, near the outer edge saddles that separate consecutive vortices.

Fine-scale turbulence indicating function

In order to perform the FSTIF analysis, the raw velocity data is transformed by, first, obtaining the time second derivative of each velocity signal and, second, computing its envelope, and storing these FSTIF signals in a separate file. After, the raw data is analysed by means of PR, and during the last iteration a record of the time locations of the individual events selected to make the velocity ensemble average is taken. This information is used to obtain the ensemble average of the FSTIF signals associated to each event that contributed to the velocity ensemble average. In this way, the FSTIF footprint corresponds unequivocally with the velocity ensemble average.

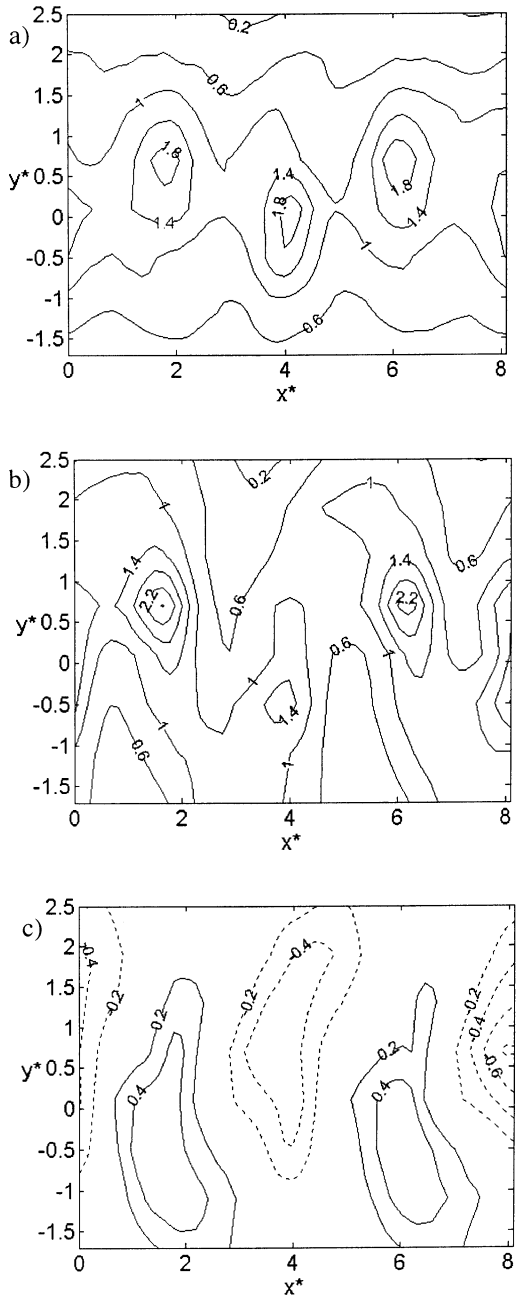

Figure 4: Incoherent components, a) $< u_r^2 >$, b) $< v_r^2 >$ and c) $< uv_r >$

Figure 5 displays the result of such analysis using the FSTIF based on the *u*-velocity component. The fine-scale activity appears again centred on the Karman vortices presenting a distribution very similar to $< u_r^2 >$ in shape, which is consistent with the fact that the velocity signal used to compute FSTIF is the streamwise component (*u*) of the velocity vector. Obviously, the contour levels in figures 4a and 5 have different values because they

correspond to different variables. No further effort has been made to find a quantitative equivalence between these two variables, since the goal of this paper is to compare the response of both methods to the selective reduction of the high frequency (fine-scale) content of the signals.

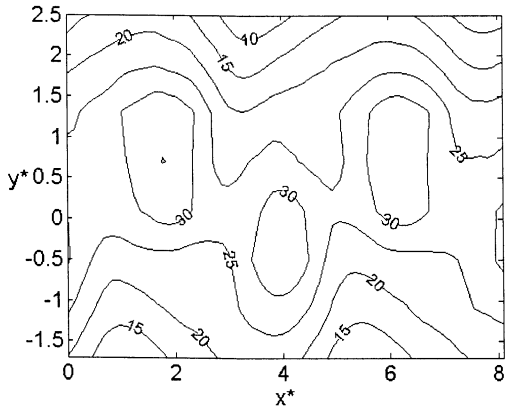

Figure 5: Fine Scale Turbulence Indicating Function

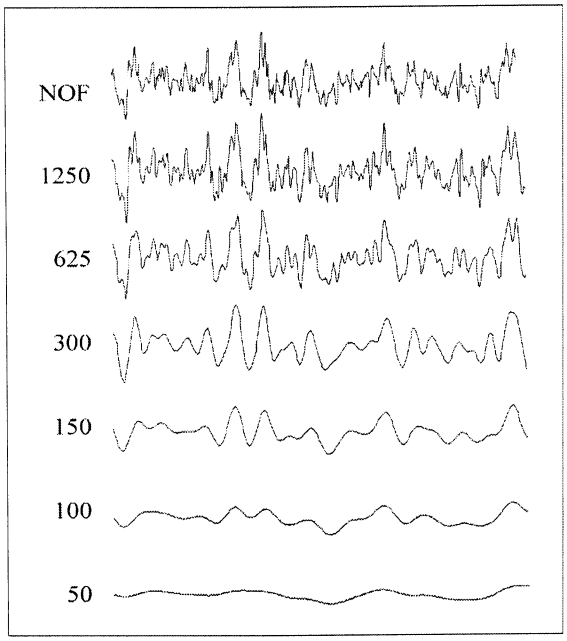

Figure 6: Sample of 100ms of data filtered using different Low-band pass filters

ANALYSIS OF FILTERED DATA

In order to compare the ability of the triple decomposition and the FSTIF in detecting the fine-scale activity of this turbulent flow, the original experimental data has been low-pass filtered at 1250Hz, 650Hz, 300Hz, 150Hz, 100Hz and 50Hz, in order to increasingly remove the fine-scale velocity fluctuations. The filter used is a symmetrical (zero lag) FIR filter. Figure 6 presents a sample of 100 ms of data filtered with the above mentioned cut-off frequencies, which can be compared to the non-filtered (NOF) data. In addition figure 3 can be re-examined now to see the positioning of the selected cut-off frequencies over the spectrum of v.

The analysis procedure outlined in the previous section has been repeated for each set of low-pass filtered data, obtaining in each case results like those already presented in figures 2, 4 and 5. To ensure that the events contributing to the ensembles averages are the same in all cases, the PR procedure has not been repeated, rather the information obtained from the original PR analysis (figure 2) has been used to take ensemble averages of velocities or FSTIF. In this way the ensemble averages obtained for all the filtered data are contributed by the same events, and the only difference between them arises from the effect of the low-pass filters that remove the fine-scale activity.

The contours and peak values of the ensemble averages of $<u_r^2>$, $<v_r^2>$ and $<uv_r>$ do not change significantly until the 150Hz filter is applied.

This is consistent with the fact that the Karman vortices are shed at 156Hz. However, the ensemble average of FSTIF does show a gradual change. For the sake of brevity these ensemble averages are not presented here, but the results of this analysis is shown in figures 7, 8 and 9. Figure 7 compares the x*-averaged profile of the FSTIF at several cut-off frequencies, while figure 8 compares the x*-averaged profiles of the $<u_r^2>$, $<v_r^2>$ and $<uv_r>$ contours.

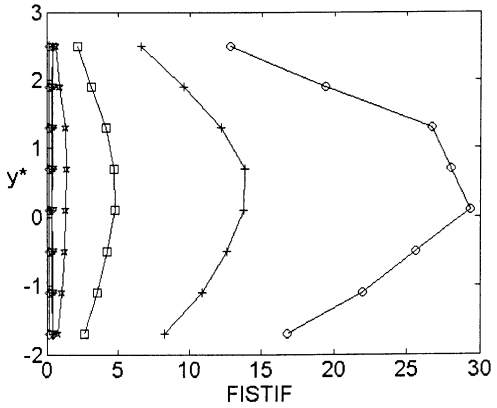

Figure 7: Profiles of FSTIF. (See legend in figure 8)

It can be observed that the reduction of the peak values of the incoherent stresses with the decreasing cut-off frequency of the low-pass filter is much less noticeable than in case of FSTIF, that almost halves its peak value as the cut-off frequency halves. This

behaviour is better observed in figure 9. Here the peak values of each profile, normalised by the peak value of the non-filtered data, are plotted against the cut-off frequency of the filter. The fine-scale stresses derived from the triple decomposition are almost unchanged by a cut-off frequency of 650Hz, for example, while the FSTIF peak is below 20% of its maximum value attained with the non-filtered data.

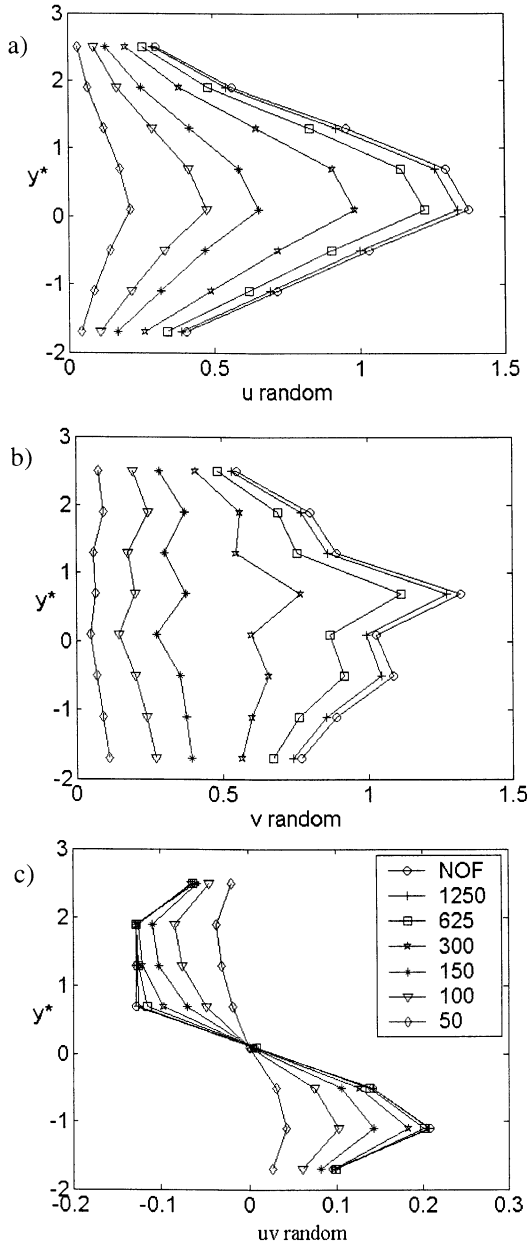

Figure 8: Profiles of the incoherent components, a) $<u_r^2>$, b) $<v_r^2>$ and c) $<uv_r>$ for no filtered data (NOF) to 50Hz filter.

The different behaviour of these two approaches to the analysis of the fine-scale activity is still enhanced if figure 9 is compared with the portion of the spectrum that is effectively removed by the low-pass filters (see figure 3).

Another fact that has to be taken in to account is that the data analysed corresponds to the near wake of a cylinder at x/D=16, a region where the Karman vortices are still fairly periodic and regular in shape an intensity. The behaviour of both techniques could be still more different in the far wake, where the structures show a range of sizes, intensities and lateral positions (Ferré et al., 1990).

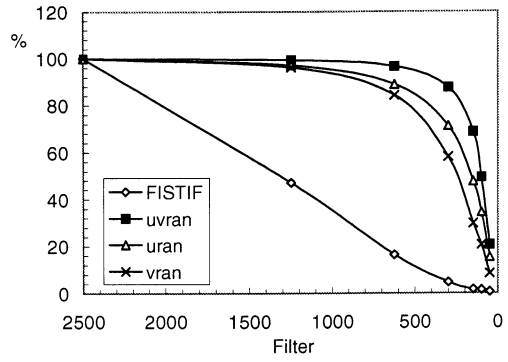

Figure 9: Absolute maximum versus filter.

FINAL DISCUSSION

Although in this flow the triple decomposition is able to qualitatively detect the zones where the fine-scale activity is concentrated, it seems to be inappropriate to yield accurate quantitative estimates of the incoherent stresses. The fact is that the differences between the individual events of one family and their ensemble average (this is what is measured with eq. 2, 3 or 4) are due both to fine-scale activity, but also to differences in size or shape of the large-scale motions averaged. Therefore, the random stresses as computed by eq. 2, 3 and 4 have indistinguishable contributions from both true fine-scale activity and the large-scale non-homogeneity. Moreover, the results presented in figure 9 suggest that most of this contribution to the random stresses comes from the larger scales. This can be inferred form the fact that a low-pass filter with a cut-off frequency of 650Hz lefts almost unchanged the peak values of $<u_r^2>$, $<v_r^2>$ and $<uv_r>$, and the maximum reduction attained with a cut-off frequency of 300Hz just lowers $<v_r^2>$ to 60% of its maximum. None of these values are consistent with the frequency content of the v-signal displayed in figure 3, and the conclusion is that the so-called random stresses are not as random (fine-scale) as they intend to be.

Because FSTIF is computed independently of the ensemble average, it is not influenced by the differences in size or shape of the large-scale motions. Note that a cut-off frequency of 1250Hz, that certainly would only affect the finer scales, but not the $\overline{u^2}$, reduces the FSTIF peak value to 50%. A

further halving of the cut-off frequency to 650Hz lowers the peak value of the FSTIF to less than 20%, and after eliminating the whole inertial range, with a low-pass filter at 300Hz, FSTIF goes to only the 5% of the non-filtered maximum. This is the expected behaviour of a fine-scale turbulence indicating function. The final conclusion is that the performance of FSTIF in detecting the fine-scale activity of this flow is much better than that of the random stresses derived from the triple decomposition.

ACKNOWLEDGES

We will like to thank Dr. G. A. Kopp, now at the Boundary Layer Wind Tunnel Laboratory of the Western Ontario University, Canada, for providing his experimental data. This work was financially supported by project DPI2000-1578-C02-01.

REFERENCES

Antonia, R.A., Browne, L.W.B., Bisset, D.K. and Fulachier, L., 1987, "A description of the organized motion in the turbulent far wake of a cylinder at low Reynolds number", *J. Fluid Mech.* Vol. 184, pp. 423-444.

Ferré, J.A., Giralt, F., 1989, "Pattern-recognition analysis of the velocity field in plane turbulent wakes", *J. Fluid Mech.* Vol. 198, pp. 27-64.

Ferré, J.A., Mumford, J.C., Savill, A.M. and Giralt F.,1990, "Three-dimensional large- eddy motions and fine-scale activity in a plane turbulent wake", *J. Fluid Mech.* Vol. 210, pp. 371-413.

Hussain, A.K.M.F., 1983, "Coherent structures - reality and myth", *Phys. Fluids* Vol. 26, pp. 2816-2850.